Cubic-phase function evaluation for multicomponent signals with application to SAR imaging

Igor Djurović, Cornel Ioana, Thayananthan Thayaparan, LJubiša Stanković, Pu Wang, Vesna Popović, Marko Simeunović

Abstract— **A cubic-phase function evaluation technique for multicomponent FM signals with non-overlapped components in the TF plane is proposed. The proposed technique is based on the STFT. Cross-terms are removed or reduced in the same manner as in the case of the TF representation called the S-method. The proposed technique is applied for visualization of signals in time-chirp-rate plane and parameter estimation of analytical and radar signals. In addition, a procedure for focusing SAR images by using estimated parameters is proposed in order to verify obtained results.**

I. Introduction

The polynomial phase signals (PPS) are observed in numerous research fields: radar, sonar, biomedicine, seismology signals, etc. [1]-[3]. The cubic-phase function (CPF) has been recently introduced for estimation of cubic-phase signals and it is generalized for higher-order PPS [4]-[8]. This is a bilinear transformation that performs mapping of signals into time-chirp-rate (T-CR) plane. Due to its bilinearity, this transform suffers from the cross-terms and interferences. It should be noted that "geometry" of interferences in this representation is still unknown as oppose to the classical time-frequency (TF) representations [9], [10].

In this manuscript, we propose a technique for calculating the CPF in the frequency domain. This technique allows to separate the CPF of signal components that are non-overlapped in the TF plane. It is applied to the parameter estimation of the Synthetic Aperture Radar (SAR) signals. In the SAR systems, radar return from a target with constant velocity or accelerating target is linear frequency modulated (FM) or cubic phase signal [11]. As a result of these modulations, moving targets are defocused in the radar image obtained by using the two dimensional (2D) Fourier Transform (FT) [12]. Therefore, the proposed technique is attractive for application to SAR imaging. Namely, by the proposed technique the CPF can be calculated separately for each signal component (target) and the estimated parameters used for its demodulation. Then, the focused SAR image can be obtained as the 2D FT of resulting signals.

The paper is organized as follows. The CPF is introduced in Section II, where we present influence of the cross-terms in this representation. The proposed technique for evaluation of the CPF and Otsu algorithm for threshold determination are described in Section III. The SAR signal model is given in Section IV. Numerical examples for both, analytical and radar signals are presented in Section V and VI, respectively. Conclusions are given in Section VII.

II. Cubic-phase function

The CPF introduced by O'Shea is defined as [4]:

$$C(t,\Omega)=\int_{-\infty}^{\infty} x(t+\tau)x(t-\tau)e^{-j\Omega\tau^2}d\tau, \quad (1)$$

where we consider the FM signal $x(t) = A\exp(j\phi(t))$. The CPF has a form similar to the Wigner distribution (WD) [10]. The WD is used for the instantaneous frequency (IF)

estimation, where the IF is the first derivative of the signal phase function $\omega(t) = \phi'(t)$. The CPF can be used as the chirp-rate estimator, where the chirp-rate is defined as the second derivative of the signal phase, i.e., $\Omega(t) = \phi''(t)$, as:

$$\hat{\Omega}(t) = \arg\max_{\Omega} |C(t,\Omega)|. \tag{2}$$

Consider now a multicomponent signal $x(t) = \sum_i x_i(t) = \sum_i A_i \exp(j\phi_i(t))$. The CPF of this signal can be written as:

$$C(t,\Omega) = \sum_i C_i(t,\Omega) + \sum_{\substack{i,j \\ i\neq j}} C_{ij}(t,\Omega), \tag{3}$$

where $C_{ij}(t,\Omega)$ are cross-terms caused by mutual influence of different signal components:

$$C_{ij}(t,\Omega) = \int_{-\infty}^{\infty} x_i(t+\tau)x_j(t-\tau)e^{-j\Omega\tau^2}d\tau. \tag{4}$$

However, eliminating (or reducing) cross-terms is just part of solution. Namely, the CPF is complex-valued, oscillatory and its absolute value is ideally concentrated on the chirp-rate for cubic-phase signals. It can be approximately written as $C_i(t,\Omega) \approx A_i^2 \exp(j2\phi_i(t))\delta(\Omega - \phi_i''(t))$ and for multicomponent signals, even with reduced cross-terms $C_{ij}(t,\Omega)$, we still have highly oscillatory representation. Then, our goal here is primarily to obtain specific components $C_i(t,\Omega)$.

III. Proposed approach

A. Evaluation of the CPF

In this section, a new approach to evaluate the CPF in the frequency domain is proposed. It requires the short-time Fourier transform (STFT), which is defined as:

$$STFT(t,\omega) = \int_{-\infty}^{\infty} x(t+\tau)w^*(\tau)e^{-j\omega\tau}d\tau. \tag{5}$$

It is noted that the STFT is a linear transform and cross-terms between components can appear only in the case when they are very close to each other (within window width in the frequency domain) [13]. The inverse STFT can be written as:

$$x(t+\tau) = \frac{1}{2\pi w^*(\tau)} \int_{-\infty}^{\infty} STFT(t,\omega)e^{j\omega\tau}d\omega. \tag{6}$$

For the sake of simplicity, we assume that the window function within the interval of interest is equal to 1. After substituting (6) in (1) we obtain (unimportant multiplicative constants are removed):

$$\begin{aligned} C(t,\Omega) &= \int_{-\infty}^{\infty}\int_{-\infty}^{\infty}\int_{-\infty}^{\infty} STFT(t,\omega_1)STFT(t,\omega_2) \\ &\quad \times e^{j(\omega_1-\omega_2)\tau}e^{-j\Omega\tau^2}d\tau d\omega_1 d\omega_2 \\ &= \int_{-\infty}^{\infty}\int_{-\infty}^{\infty} STFT(t,\omega_1)STFT(t,\omega_2) \\ &\quad \times \Pi_\Omega(\omega_2-\omega_1)d\omega_1 d\omega_2 \\ &= \int_{\omega}\int_{\theta} STFT(t,\omega+\theta)STFT(t,\omega-\theta) \\ &\quad \times \Pi_\Omega(2\theta)d\omega d\theta, \end{aligned} \tag{7}$$

where $\Pi_\Omega()$ is the FT of the linear FM signal $\exp(-j\Omega\tau^2)$:

$$\Pi_\Omega(\theta) = \int_{-\infty}^{\infty} e^{-j\Omega\tau^2}e^{-j\theta\tau}d\tau. \tag{8}$$

The implementation of the CPF in (7) in the T-CR domain is a counterpart of the TF transform called the S-method [13], [14].

Assume now that a significant energy of any signal component exists only within the frequency region $[\omega_{bi}(t), \omega_{ei}(t)]$, and that signal components are non-overlapping in the TF plane, i.e., $[\omega_{bi}(t), \omega_{ei}(t)] \cap [\omega_{bj}(t), \omega_{ej}(t)] = \varnothing$ for $i \neq j$. Then, the CPF for the $i-$th signal component can be written as:

$$\begin{aligned} C_i(t,\Omega) &= \\ &\iint_{\omega_{bi}(t)\leq\omega\pm\theta\leq\omega_{ei}(t)} STFT(t,\omega+\theta)STFT(t,\omega-\theta) \\ &\quad \times \Pi_\Omega(2\theta)d\omega d\theta, \end{aligned} \tag{9}$$

or for discretized frequencies as:

$$C_i(t,\Omega)=\sum_{k=k_i'}^{k_i''}\Big[STFT_i^2(t,k)\Pi_\Omega(0)$$

$$+2\sum_{l=1}^{\min[k_i''-k,k-k_i']}STFT_i(t,k+l)STFT_i(t,k-l)$$

$$\times\,\mathrm{Re}\{\Pi_\Omega(2l)\}\Big]. \qquad (10)$$

Here, the discretized frequencies correspond to $\omega_{bi}=2\pi k_i'/(N\Delta t)$ and $\omega_{ei}=2\pi k_i''/(N\Delta t)$, where Δt is sampling rate and N is number of samples in the considered interval. In this way, the evaluation of the CPF for the i-th component $C_i(t,\Omega)$ is separated from evaluation of the CPF for other components.

Determination of region of the signal components is not easy and it heavily depends on the considered signal type. For this aim we used the Otsu algorithm [15], already applied for radar signal segmentation in [16]. This algorithm exhibits high accuracy in the considered application.

B. Otsu algorithm

The Otsu algorithm is one of the simplest and most commonly used techniques for threshold determination in the image processing field [15]. This algorithm has already been used in TF analysis for separating signal components from radar returns [16]. In our case, we select the initial threshold as $T=\max_{(t,\omega)}[|STFT(t,\omega)|]/2$. Then, the mean value of the $|STFT(t,\omega)|$ "pixels" that are above the threshold (T_1) and mean value of the $|STFT(t,\omega)|$ "pixels" that are below the threshold (T_2) are evaluated. Average of these two quantities is used as a threshold for a new iteration $T=(T_1+T_2)/2$. Iterations are repeated until a difference between thresholds in two consecutive iterations is not below specific value or for specific number of iterations. This technique is used for threshold determination and region above the threshold could be assumed to belong to signal component. Positions $\omega_{bi}(t)$ and $\omega_{ei}(t)$ are determined as the beginning and the end of the continuos region above the threshold. It works accurately in the noise-free examples for analytical and SAR signals. However, for high amount of noise, the Otsu algorithm could produce a large number of fake components. Let the detected regions of these components be denoted as $[\omega_{bi}(t),\omega_{ei}(t)]$, $i\in[1,Q]$, where Q is number of detected components. Some of detected components are fake. Therefore, it can be assumed that the number of signal components P, that is in general $P\leq Q$, is known in advance. Then, one can determine the energy concentrated in the signal component:

$$E_i(t)=\int_{\omega_{bi}(t)}^{\omega_{ei}(t)}|STFT(t,\omega)|d\omega, \qquad (11)$$

and select P intervals with the highest energy for which the CPF is evaluated. In addition, we have found that for high amount of noise the Otsu algorithm tends to reduce the width of detected signal components. Therefore, we set the minimal width of signal component and dilate region detected in the Otsu procedure until we reach this minimal width [15, pp. 343]. In the considered radar applications this threshold selection procedure produces accurate results. Depending on the signal type and noise environment, modified version of the threshold selection technique can be required. Fortunately, the digital image processing area offers several quite successive techniques for separation of objects from noisy background [15].

IV. SAR SIGNAL MODEL

The SAR is a system for obtaining high resolution radar image based on a relative angle change of the radar with respect to a target. In the SAR systems, a radar is carried on a platform moving with uniform speed at constant altitude [12]. Along-track direction is called the cross-range (azimuth), while across-track direction is the range. The SAR images are depicted in the range/cross-range domain.

Usually, for modeling radar signal, the point scatterer model is used [12]. Then, received signal, after some preprocessing, can be writ-

ten as a sum of FM signals [12]:

$$q(m,n)=\sum_i \sigma_i e^{j\phi_i(m,n)}, \qquad (12)$$

where σ_i is reflection coefficient of the corresponding scatterer, while m corresponds to the signal number transmitted toward a target (slow-time coordinate), and n corresponds to the sample number within a one chirp (fast-time coordinate). Form of the phase functions $\phi_i(m,n)$ depends on the type of the corresponding radar scatterer.

Standard tool for SAR imaging is the 2D FT. In the case when the SAR targets are nonmoving, radar signal is composed of a sum of complex sinusoids and image obtained by using the 2D FT is well focused [12]. For moving targets, the corresponding radar signal is composed of linear FM signals. Moreover, when the motion of a target is nonuniform along the cross-range, the third order term in the corresponding phase is significant and cannot be neglected [11]. As a consequence of the signal phase modulations, induced by its motion, targets will be defocused and possibly shifted in the SAR image obtained by using the 2D FT [12]. Hence, some more sophisticated techniques are needed for focusing radar images of moving targets.

Commonly, spreading in the SAR systems occurs only in the cross-range domain [12] and we are performing autofocusing operations only in this domain. Thus, we need to estimate parameters of discrete signal $x(m)$ representing the radar signal for fixed n, i.e., $x(m)=q(m,n)$. In order to perform calculations for smaller number of ranges, we could estimate parameters of radar signal by using the CPF only for those ranges in which there is one or more moving targets. Then, higher order terms from the phase of each component can be removed by using estimated parameters and SAR image obtained as the 2D FT of demodulated signal. Achieved concentration of the resulting SAR image would be proportional to the accuracy of parameters estimation, and it presents a good measure of accuracy of the proposed technique.

V. Numerical examples

Example 5.1. Sum of three linear FM signals:

$$x(t)=e^{j(-30\pi t^2-72\pi t)}+e^{j(30\pi t^2+72\pi t)} +e^{j(26.1\pi t^2+160\pi t+0.34\pi)}, \qquad (13)$$

is considered. The signal is given within the interval $t\in[-0.4,0.4]$ with sampling rate $\Delta t=1/257$. Fig. 1 depicts results of the algorithm. The STFT and selected region of interest are depicted in Figs. 1a,b. The CPF calculated by using the standard definition is presented in Fig. 1c. Two close components (second and third) cannot be clearly distinguished and in addition there are oscillations caused by mutual interaction between "auto-terms". The CPF estimates obtained by using (10) for our three signal components are given in Figs. 1d-f. The chirp-rate estimation for the first component is given in Fig. 1g, while for the two close components it is given in Fig. 1h. For a given component, chirp-rate is estimated as a position of the corresponding CPF maximum:

$$\hat{\Omega}_i(t)=\arg\max_{\Omega}|C_i(t,\Omega)|. \qquad (14)$$

The differences between true and estimated chirp-rates in Fig. 1g are caused by discretization of the set of chirp-rate values (errors within one discretization step). From these figures it can be noted that the proposed approach behaves accurately for this setup.

Example 5.2. Sum of two nonlinear FM signals

$$x(t)=e^{j(16\pi t^4+12\pi t^2+80\pi t)} +e^{j(-16\pi t^4-12\pi t^2-80\pi t)} \qquad (15)$$

is considered in this example. Interval of interest and sampling rate are the same as in the previous example. Fig. 2a depicts the STFT, while Fig. 2b presents the CPF calculated using the standard definition. The CPF for two detected components is depicted in Figs. 2c,d. Fig. 3 presents the estimated chirp-rates (thick lines) and true chirp-rate values $\Omega_{1,2}(t)=\pm(192\pi t^2+24\pi)$ (thin lines). It can be seen small bias that is inherent in the CPF for higher-order PPSs (with polynomial order

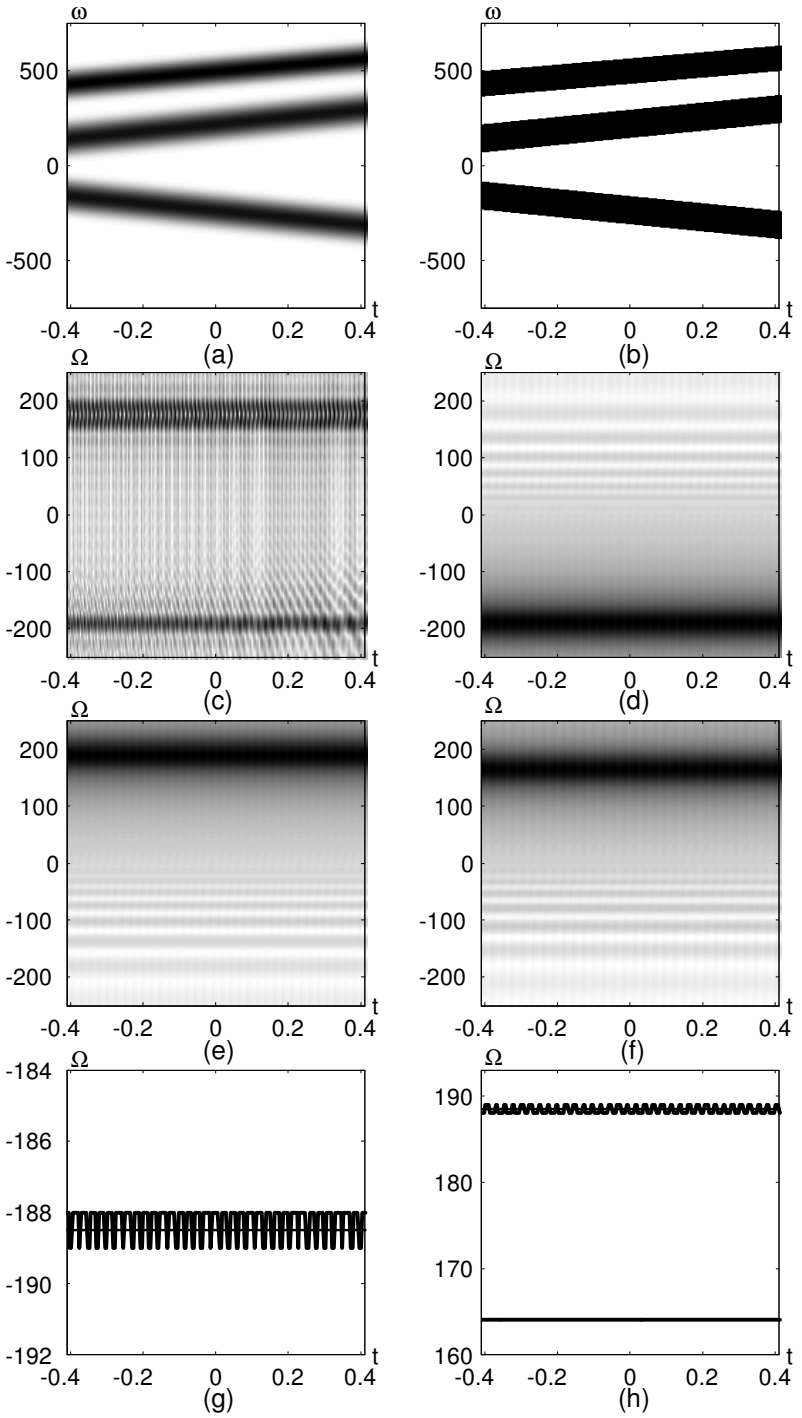

Fig. 1. Sum of three linear FM signals: (a) STFT; (b) Detected region of signal components using the Otsu algorithm; (c) Standard CPF; (d) CPF calculated using the proposed approach for the first signal; (e) CPF calculated using the proposed approach for the second signal; (f) CPF calculated using the proposed approach for the third signal; (g) Chirp-rate estimation using the proposed technique (thick line) and true chirp-rate (thin line) for the first component; (h) Chirp-rate estimation using the proposed technique (thick line) and true chirp-rate (thin line) for the second and third component.

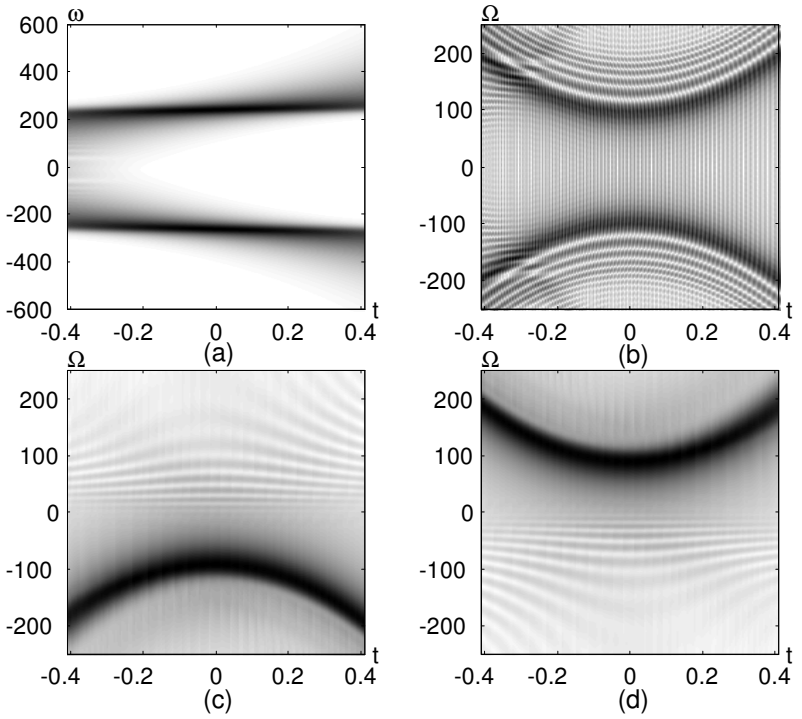

Fig. 2. Sum of non-linear FM signals: (a) STFT; (b) CPF calculated using the standard definition; (c) CPF calculated using the proposed approach for the first signal; (d) CPF calculated using the proposed approach for the second signal.

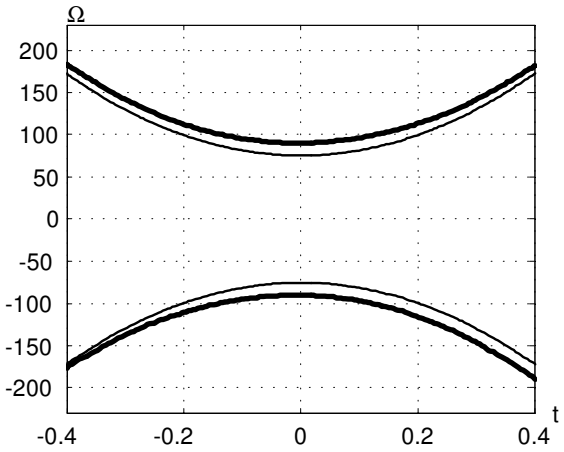

Fig. 3. Chirp-rate estimate for non-linear FM components (thick line) and true chirp-rate (thin line).

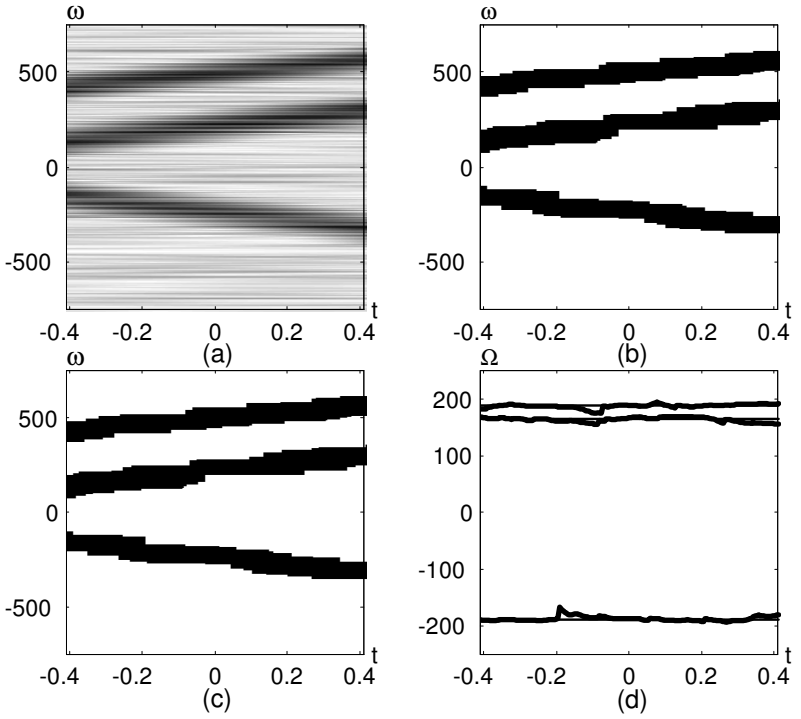

Fig. 4. Sum of three linear FM signals embedded in Gaussian noise: (a) STFT; (b) Detected region of signal components; (c) Improved detection of signal components; (d) Chirp-rate estimates obtained using the proposed technique (thick line) and true chirp-rate values (thin line) for signal components.

higher than 3) and it is not caused by our evaluation technique.

Example 5.3. The sum of linear FM signals (13) embedded in white complex Gaussian noise environment with variance equal to 1 is considered here. The STFT and region of interest are depicted in Figs. 4a,b. The modified region of signal component with removed fake components and enlarged signal components (any detected signal component is set to the minimum width of 17 samples) is depicted in Fig. 4c. Chirp-rate estimates with true chirp-rate values for the signal components are depicted in Fig. 4d. Standard deviation of the output error is about 9 and we can assume that it is still reasonable. The MSE error of the chirp-rate estimation for this signal is depicted in Fig. 5. Input SNR is measured for a single considered component (all three components have the same amplitude). Detector threshold is somewhere about -1.5dB, but again we should stress that our goal was neither to perform a thorough numerical study of the algorithm nor to propose algorithm for detection and segmentation of components in the TF plane, but to show that the proposed approach for evaluation of the CPF can work for multicomponent signals embedded in noise environment and consequently in a realistic radar scenario.

VI. SAR signal examples

Example 6.1. In this example we apply the proposed technique to the parameter estimation of the SAR signals. The CV 580 SAR system (C-band) parameters are used. The aircraft with a radar is moving along x-axis with velocity $V = 130\,\mathrm{m/s}$. Radar altitude is $h = 6\,\mathrm{km}$, while radar ground distance to the origin of the Cartesian coordinate system at time $t = 0$ is $10\,\mathrm{km}$. Radar pulses are transmitted at regular intervals in time given by the pulse repetition time $T = 1/300\,\mathrm{s}$, with $M = 1024$ pulses in one revisit. Number of

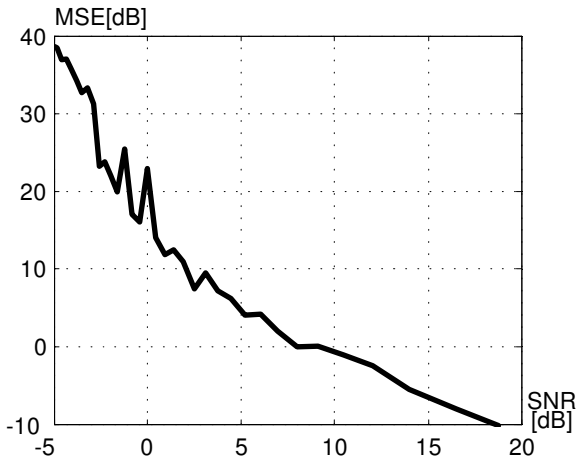

Fig. 5. MSE of chirp-rate estimation of multicomponent signals.

samples within a one pulse is $N = 1024$ like in [11]. The radar operates at the frequency $f_0 = 5.3\,\mathrm{GHz}$. The bandwidth of linear FM signals is $B = 25\,\mathrm{MHz}$.

The radar scene is composed of three targets at the same position along range direction. Its initial positions along cross-range direction are $x_{01} = -150\,\mathrm{m}$, $x_{02} = 0\,\mathrm{m}$ and $x_{03} = 150\,\mathrm{m}$, respectively. The targets are moving with cross-range accelerations: $a_{x1} = 2.4\,\mathrm{m/s^2}$, $a_{x2} = 0.6\,\mathrm{m/s^2}$ and $a_{x3} = 2.2\,\mathrm{m/s^2}$. As a result of cross-range acceleration, the corresponding radar signals have significant third order coefficients in the phase [11]. Received signal, for a range in which the targets are positioned, is composed of three cubic phase components. Since we do not intend here to form radar image, but to show accuracy of the proposed technique in the parameters estimation of the SAR signals, we analyze radar signal for this fixed range. For separating signal components in the TF plane we use the previously described Otsu based algorithm. The targets are well separated in the TF plane, therefore we use minimal region size of 16 samples in order to enhance accuracy of the applied technique. The results are still quite accurate even without this modification. Fig. 6 depicts the results obtained after the proposed technique is applied. The STFT is shown in Fig. 6a, while Fig. 6b represents regions with detected signal components. Each region corresponds to one target. The CPF estimates obtained by using the proposed approach for each detected component are given in Figs. 6c-e. Estimated chip-rate values for each signal component (thick lines) and their true values (thin lines) are shown in Fig. 6f. The true values are obtained by applying the proposed technique on the signal that consists only of the target of interest. The targets are well separated in TF plane, consequently, estimated coefficients are equal to their true values. It can be concluded that the proposed algorithm produces good results in the parameters estimation of radar signals even in the case when there is more than one target in a range bin.

Example 6.2. This example assumes the same radar parameter as in Example 6.1. The radar scene is composed of five targets with initial positions and motion parameters given in Table I. The first target is stationary, and it is well focused in the radar image obtained by using the 2D FT (Fig. 7a). Radar signals that correspond to targets No. 2 and No. 4 are cubic phase, while resulting radar signals for the targets No. 3 and No. 5 are linear FM. As a result of frequency modulation, these targets are defocused in the SAR image (Fig. 7a). A simple procedure for focusing SAR images is then used. Since, there is no defocusing along range direction, the FT is calculated along fast-time

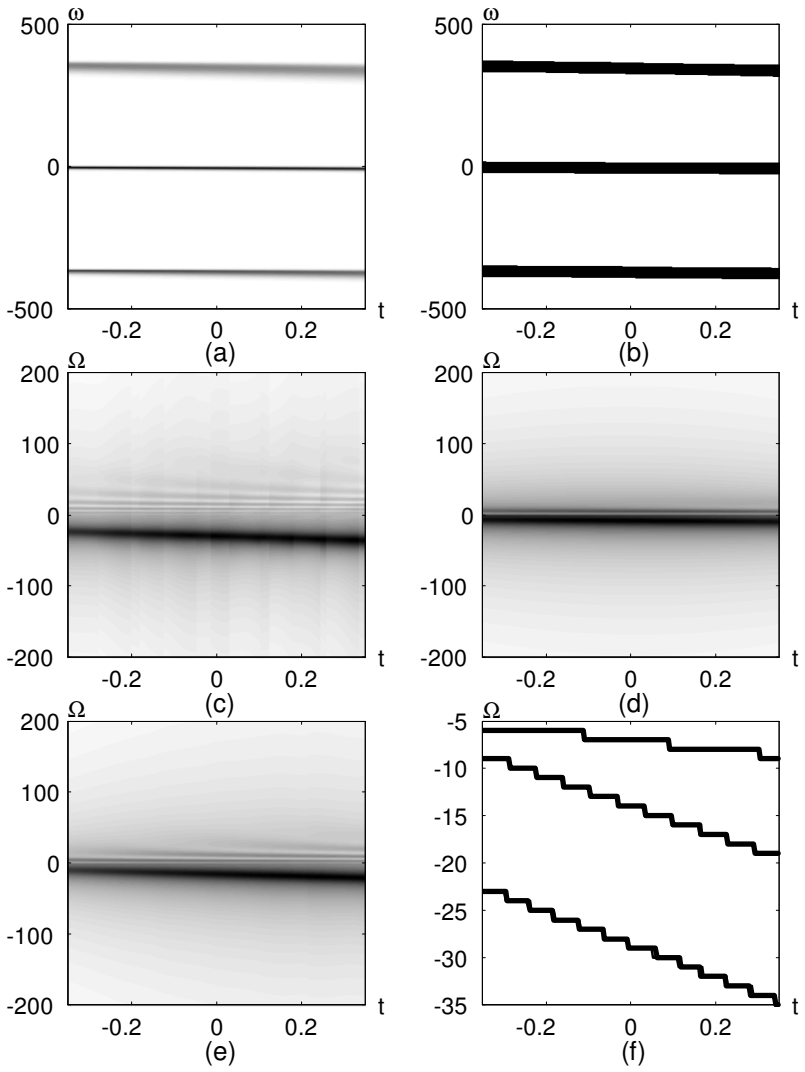

Fig. 6. Radar signal with three components with phase degree of 3: (a) STFT; (b) Detected region of signal components using the Otsu algorithm; (c) CPF calculated using the proposed approach for the first component; (d) CPF calculated using the proposed approach for the second component; (e) CPF calculated using the proposed approach for the third component; (f) Chirp-rate estimations obtained using the proposed technique (thick line) and true chirp-rate values (thin line) for signal components.

in order to obtain information about range position of the targets. For each range, the FT is calculated along slow-time and compared to a threshold obtained by using the Otsu algorithm. If the absolute value of the FT for a certain range is above the threshold, there is one or more targets in it. Then, the proposed technique is applied in order to estimate parameters of the corresponding signal. The same minimal region size as the one in the previous example is used here. The number of regions detected in TF plane is shown to be equal to the number of targets in the observed range. Therefore, the same technique is applied for detection and regions segmentation in the frequency domain. The FT calculated for this range is used in the Otsu algorithm for threshold determination. Number and order of de-

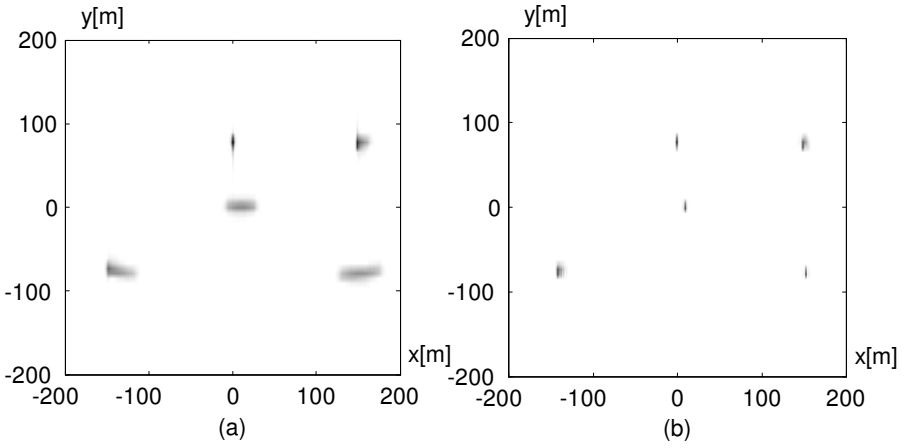

Fig. 7. SAR image of five targets: (a) obtained by using the 2D FT; (b) after focusing by using parameters estimated by the proposed technique.

tected regions is shown to be the same as the one obtained in the TF domain. Thus, each detected region is extracted from the mixture and its inverse FT is calculated in order to obtain the corresponding signal. Then, the obtained signal is dechirped by using mean value of the corresponding chirp-rate estimated by the proposed technique. The radar image, depicted in Fig. 7b, is obtained as a sum of radar images of demodulated detected returns. It can be seen, that high concentration of moving targets is obtained, without defocusing the stationary one (No. 1), that is already well focused in the 2D FT (Fig. 7a). This is good validation of the accuracy of the proposed technique for parameters estimation of radar signals.

Example 6.3. Performance of the proposed technique applied to SAR signals in the presence of noise is examined in this example. The same radar setup as the one in the previous example is considered. The radar signal is embedded in white complex Gaussian noise environment with a standard deviation equal to 10. Radar image obtained by using the 2D FT is depicted in Fig. 8a. Radar image obtained by applying the same procedure as the one described in the previous example is depicted in Fig. 8b. By comparing these two figures, it can be concluded that the proposed procedure successfully performs focusing of all targets even in the presence of noise. Moreover, it can be seen that, by the proposed procedure, significant portion of noise is rejected from the SAR image.

Example 6.4. The 2D FT of radar data produces samples (intensities of a radar image) distributed on a polar grid (R, θ), [17]. These samples correspond to intensities of the SAR image in the range/cross-range plane (the Cartesian coordinate system) along a straight-line at an angle θ from the range direction. For a far-field radar scenario analyzed in Examples 6.2-6.3 these lines could be considered to be parallel. Therefore, an error induced by depicting SAR image, obtained by using the 2D FT, in the Cartesian coordinate system is very small [17]. However, for near-field radar scenarios, this error cannot be neglected. Thus, in this example, a near-field scenario is used. The same radar setup as the one in the previous examples is considered, except that the radar altitude is 1 km, while radar ground distance to the origin of the Cartesian coordinate system at time $t = 0$ is 3 km. In addition, number of samples within a one pulse is $N = 256$, while there is $M = 256$ pulses in one revisit. The radar scene is composed of six targets with initial positions and motion parameters given in Table II.

As a result of motion they are performing, targets could be dislocated from the proper po-

TABLE I
MOTION PARAMETERS FOR THE TARGETS USED IN EXAMPLES 6.2 AND 6.3.

Scatterer No.	1	2	3	4	5
x_0 [m]	0	150	0	-150	150
y_0 [m]	90	90	0	-90	-90
v_x [m/s]	0	0	6	0	8
a_x [m/s^2]	0	2.2	0	2.4	0

TABLE II
MOTION PARAMETERS FOR THE TARGETS USED IN EXAMPLE 6.4.

Scatterer No.	1	2	3	4	5	6
x_0 [m]	-54	54	-54	54	-54	54
y_0 [m]	90	90	0	0	-90	-90
v_x [m/s]	12	0	10	0	12	14
a_x [m/s^2]	1	0	0.5	0	0	0

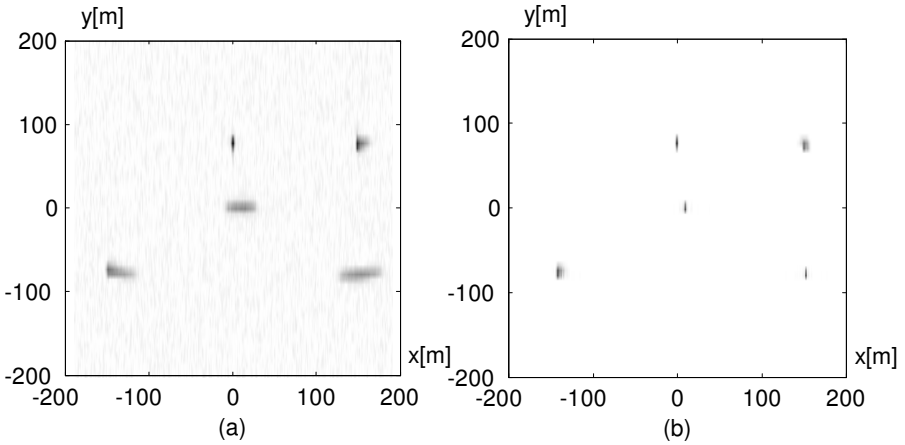

Fig. 8. SAR image of five targets embedded in white complex Gaussian noise: (a) obtained by using the 2D FT; (b) after focusing by using parameters estimated by the proposed technique.

sition in the SAR image [12]. Thus, in order to examine an error induced solely by depicting a SAR image, obtained by using the 2D FT, in the range/cross-range plane (instead of depicting it in polar coordinate system), all targets are considered to be stationary in the first part of this example. Their positions in the SAR image therefore should coincide to the positions given in Table II. The SAR image, obtained by using the 2D FT, is depicted in Fig. 9a. The targets with equal cross-range coordinate are on a radial line, instead of straight line, i.e. they are not at the true positions. One of the widely used methods for obtaining image intensities in the Cartesian coordinate system from its projection on a straight-line at an angle θ from $x-$axis is convolution back projection (CBP) image reconstruction method [18]. Details of the CBP can be found in [18]. The SAR image obtained by using the CBP method is shown in Fig. 9b. It is obtained in the Cartesian coordinate system. Targets with the same cross-range coordinate are on a straight line, i.e. at the true positions. The center of coordinate systems used for depicting SAR images given in Figs.

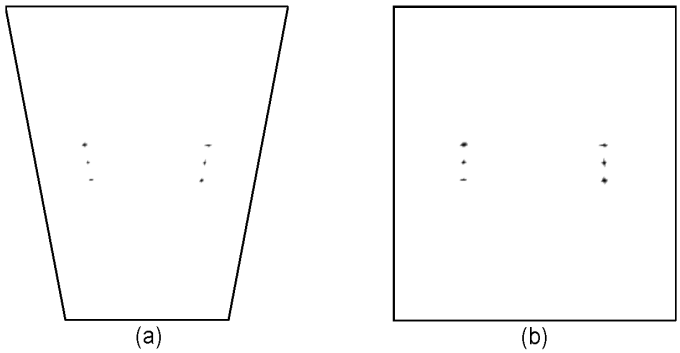

Fig. 9. SAR image obtained by using: (a) the 2D FT, depicted in corresponding polar coordinate system; (b) the CBP image reconstruction method, depicted in the Cartesian coordinate system.

9a,b coincide to the ground projection of the radar position at $t = 0$. A part of a polar coordinate system $\theta \in [-1.8715^o, 1.8715^o]$ and $R \in [2.1905\,\text{km}, 3.8032\,\text{km}]$ is depicted in Fig. 9a.

In the second part of this example, the targets with motion parameters given in Table II are considered. As a result of motion, some of the targets are defocused in the SAR image shown in Fig. 10a. Here, the SAR image is obtained by using the CBP image reconstruction method. The radar image obtained by applying the same procedure as the one described in the previous SAR examples is depicted in Fig. 10b. The CBP image reconstruction method is used here, as well, in order to obtain the final SAR image in the range/cross-range plane. One can see that performance of the proposed technique is independent of the CBP image reconstruction method. The proposed technique successfully performs focusing of all targets, while by using the CBP image reconstruction method, their positions are obtained in the Cartesian coordinate system, instead of polar one. These two parts of procedure for forming a final SAR image can be performed separately. Namely, the aim of the proposed algorithm for SAR imaging is to demodulate a radar signal (in order to remove higher order phase terms) by using parameters estimated by the CPF. Then, the obtained (demodulated) radar signal can be used in the CBP algorithm for radar imaging.

VII. Conclusions

The CPF evaluation technique for multicomponent signals is presented. The proposed technique is based on the STFT. Accuracy of the proposed approach is demonstrated for sum of linear FM signals, sum of nonlinear FM signals, and for noisy signals. Moreover, it is applied to the parameters estimation in the case when motion performed by the targets in SAR systems induces the second and third order terms in the phase of the corresponding signals. The proposed technique produces good results in these cases. Significant direction in further research is problem of components overlapping in the TF plane. Our current investigation are going in direction of projection based techniques. Furthermore, the proposed technique should be combined with an appropriate technique for detection and segmentation of signal components in the TF plane.

VIII. Acknowledgement

The work of Igor Djurović was realized at the INP Grenoble, France, and supported by the French CNRS, under contract No. 180 089 013 00387. This research was supported in part by the Ministry of Science and Education of Montenegro. The work of Pu Wang was supported by the National Natural Science

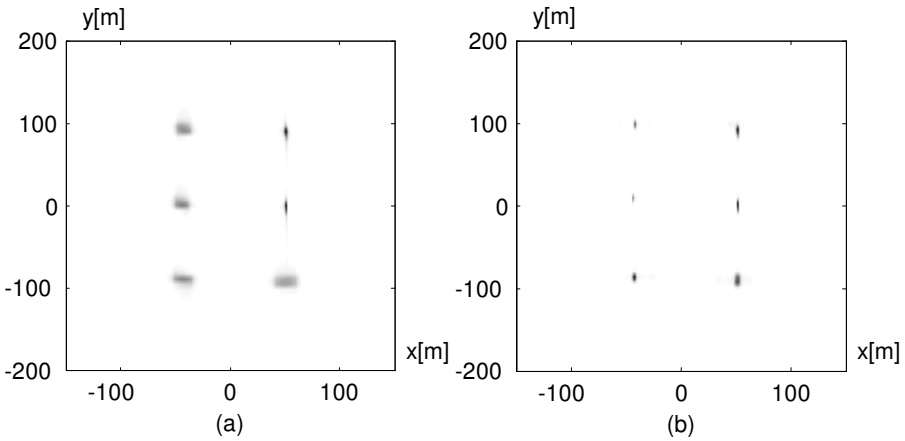

Fig. 10. SAR image of six targets: (a) the CBP image reconstruction method; (b) after focusing by using parameters estimated by the proposed technique with the CBP image reconstruction method.

Foundation of China under Grant 60802062.

References

[1] Porat, B.: 'Digital processing of random signals: Theory and methods' (Englewood Cliffs, NJ: Prentice-Hall, 1994).

[2] Peleg, S. and Friedlander, B.: 'The discrete polynomial phase transform', IEEE Trans. Signal Process., 1995, 8, (43), pp. 1901–1914.

[3] Reid, D.C., Zoubir, A.M. and Boashash, B.: 'Aircraft flight parameter estimation based on passive acoustic techniques using the polynomial Wigner–Ville distribution', J. Acoust. Soc. Amer., 1997, (102), pp. 207–223.

[4] O'Shea, P.: 'A fast algorithm for estimating the parameters of a quadratic FM signal', IEEE Trans. Signal Process., 2004, 2, (52), pp. 385-393.

[5] Farquharson, M. and O'Shea P.: 'Extending the performance of the cubic phase function algorithm', IEEE Trans. Signal Process., 2007, 10, (55), pp. 4767-4774.

[6] Farquharson, M., O'Shea, P. and Ledwich, G.: 'A computationally efficient technique for estimating the parameters of polynomial phase signals from noisy observations', IEEE Trans. Signal Process., 2005, 8, (53), pp. 3337-3342.

[7] O'Shea, P.: 'A new technique for instantaneous frequency rate estimation', IEEE Signal Process. Let., 2002, 8, (9), pp. 251-252.

[8] Wang, P., Djurović, I. and Yang, J.: 'Instantaneous frequency rate estimation based on robust cubic phase function', Proc. Int. Conf. on Acoustics, Speech, and Signal Processing, Toulouse, France, May 2006, pp. 89–92.

[9] Jeong, J. and Williams, W.J.: 'Mechanism of the cross-terms in spectrograms', IEEE Trans. Signal Process., 1992, 10, (40), pp. 2608-2613.

[10] Hlawatsch, F. and Boudreaux-Bartels, G.F.: 'Linear and quadratic time-frequency signal representations', IEEE Signal Process. Mag., 1992, 2, (9), pp. 21-67.

[11] Sharma, J.J., Gierull, C.H. and Collins, M.J.: 'Compensating the effects of target acceleration in dual-channel SAR-GMTI', IEE Proc. of Radar, Sonar and Navigation, 2006, 1, (153), pp. 53-62.

[12] Chen V. C. and Ling H.: 'Time-frequency transforms for radar imaging and signal analysis' (Artech House, Boston, USA, 2002).

[13] Stanković, LJ.: 'A method for time-frequency signal analysis', IEEE Trans. Signal Process., 1994, 1, (42), pp. 225-229.

[14] Stanković, LJ.: 'Quadratic and higher order time-frequency analysis based on the STFT', in Boashash, B. (Ed.): 'Time-Frequency Signal Analysis and Processing' (Elsevier, 2003), pp. 242-250.

[15] Gonzalez, R.C. and Woods, R.E.: 'Digital image processing' (Prentice Hall, 2002).

[16] Stanković, LJ., Thayaparan, T., Popović, V., Djurović, I. and Daković, M.: 'Adaptive S-method for SAR/ISAR imaging', EURASIP Journal on Advances in Signal Processing, 2008, (2008), Article ID 593216, 10 pages, doi:10.1155/2008/593216.

[17] Xiao, S., Munson, D.C., Jr., Basu. S. and Bresler, Y.: 'An N^2logN back-projection algorithm for SAR image formation', Conf. Rec. of the Thirty-Fourth Asilomar Conference on Signals, Systems and Computers, Pacific Grove, CA, USA, October 2000, (1), pp. 3-7.

[18] Desai, M.D. and Jenkins, W. K.: 'Convolution backprojection image reconstruction for spotlight mode synthetic aperture radar', IEEE Trans. Image Processing, 1992, 4, (1), pp. 505-517.